Applied Mathematics and Mechanics
(English Edition, Vol. 2 No. 4, Oct. 1981)

Published by Techmodern Busines
Promotion Centre, Hong Kong

The Motion of Viscous Liquid Column with Finite Length in a Vertical Straight Capillary Tube*

Wu Wang-yi (吴望一)
(*Department of Mechanics, Beijing University, Beijing*)
Qian Min-quan (钱民全)
(*Institute of Mechanics, Chinese Academy of Sciences, Beijing*)
Wen Gong-bi (温功碧)
(*Department of Mechanics, Beijing University, Beijing*)
(*Received on Nov. 4, 1980*)

Abstract

This paper deals with the motion of viscous liquid column with finite length and two free surfaces in a vertical straight capillary tube. It is assumed that fluid is Newtonian. Linearizing the boundary conditions, analytic expressions in the form of infinite series have been obtained for velocity, pressure and free surface at low Reynolds number. The numerical calculation is carried out for a set of cylinder's length of water and blood. It has been revealed that there are considerable circulating currents at the upper and lower meniscuses. Its maximum velocity is about 57% of the average velocity of the mainstream. Inertial effect is also studied in this paper. Using the time-dependent method in finite difference techniques, numerical solution of the corresponding nonlinear equation at $Re\leqslant 24.5$ is computed. Comparing it with analytic exact solution at low Reynolds number shows that inertial effect is negligible provided $Re\leqslant 24.5$.

I. Governing Equations and Boundary Conditions

The circles of medical science follow the mechanism of thrombus formation, which is related to many complicated physiological phenomena and hydrodynamic characteristics with great interest. In 1958, Chandler devised an apparatus of rotating circular loop. The loop made of plastic tube was rotated at a certain angular speed. A sample of whole blood flows relatively to the tube in the lower half loop. After a few minutes of rotation, an artificial thrombus was formed in vitro (see Fig. 1). Recently, M. Q. Qian developed an apparatus which

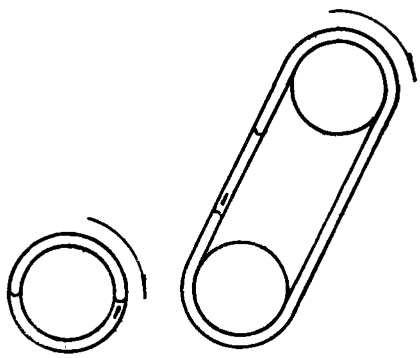

Fig. 1

* Communicated by Chien Wei-zang

we call rotating belt-loop. A loop of plastic tube was set on two pulleys like a belt. This loop was driven by a rotating pulley and a sample of whole blood flows relatively to the tube in the straight segment of the loop. After a few minutes of rotation. thrombus was also found to have formed (Fig. 1). This paper studies the motion of viscous liquid column with finite length in a vertical straight capillary tube. By means of revealing the flow characteristics near the location of thrombus formation we intend to clarify the hydrodynamical conditions for thrombus formation.

Consider the motion of liquid column of finite length in the vertical straight capillary tube under the action of gravity. Observations show that over a period of time liquid column falls at constant speed due to simultaneous action of gravity, surface tension and viscous force. For simplicity we fix the coordinate system with the liquid column descended as a whole at speed U (U is also the average speed for any profile of liquid column relative to absolute coordinate system fixed with capillary). Then the wall of capillary has an upward motion at speed U, and the motion of liquid column is steady. It is easy to imagine that as the wall of capillary moves upwards it causes the viscous fluid located at its neighbour to move upwards with it. As soon as the fluid particles reach the upper meniscus, it diverts due to occlusion and travels along the free surface. Then, changing direction, they flow further in the direction of the axis. As a result, a circulating current is formed in the upper meniscus. Similarly, we can conclude that the same circulating current exists in the lower meniscus.

Now, starting from governing equations of viscous fluid we consider the hydrodynamic characters of the circulating current in more detail. In other words we will determine its flow pattern, velocity, pressure, shear stress and form of free surface. For simplicity it is assumed that:

1) The fluid is considered as Newtonian, viscous and incompressible.

2) The fluid motion is steady.

3) The liquid layer which remains at the wall is infinitely thin.

4) There are gravity and surface tension on free surface, acting on the fluid.

Suppose the length of the fluid column is $2L$ (the intersections of the wall and the upper and lower meniscuses are taken as its starting point and end point). It is convenient to work with a columnar system of coordinates (x, r, θ), (see Fig. 2) the origin of which is located at the

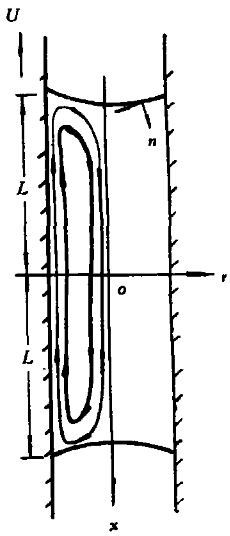

Fig. 2

centre of the liquid column. U, a, $\frac{\mu U}{a}$, μU are employed as the characteristic scales of velocity, length, pressure and surface tension. Then, we have

$$\left.\begin{array}{l} x=x'a,\ \ r=r'a,\ \ L=\lambda a, \\ u=u'U,\ \ v=v'U,\ \ p=p'\frac{\mu U}{a},\ \ \ p_a=p'_a\frac{\mu U}{a} \\ T=T'\mu U,\ \ G=\frac{ga^2}{\nu U},\ \ Re=\frac{Ua'}{\nu} \end{array}\right\} \quad (1.1)$$

where quantities with index "$'$" are dimensionless, while quantities without "$'$" are correspondingly dimensional, and they are the components of the velocity, respectively, p is pressure, T is surface tension, a is radius of capillary, p_a is atmosphere, g is acceleration of gravity, μ and ν are kinematic and dynamic viscosity respectively. The steady motion of viscous liquid column in a vertical capillary tube satisfies the following dimensionless equations and boundary conditions.

$$\left.\begin{array}{l} Re\left(u\frac{\partial u}{\partial x}+v\frac{\partial u}{\partial r}\right)=G-\frac{\partial p}{\partial x}+\frac{\partial^2 u}{\partial x^2}+\frac{\partial^2 u}{\partial r^2}+\frac{1}{r}\frac{\partial u}{\partial r} \\ Re\left(u\frac{\partial v}{\partial x}+v\frac{\partial v}{\partial r}\right)=-\frac{\partial p}{\partial r}+\frac{\partial^2 v}{\partial x^2}+\frac{\partial^2 v}{\partial r^2}+\frac{1}{r}\frac{\partial v}{\partial r}-\frac{v}{r^2} \\ \frac{\partial u}{\partial x}+\frac{\partial v}{\partial r}+\frac{v}{r}=0 \end{array}\right\} \quad (1.2)$$

$$u=-1,\ v=0 \ \text{ for } r=1 \quad (1.3)$$

$$v=0 \qquad \text{ for } r=0 \quad (1.4)$$

on the free surface $x=\mp\lambda+F_{\mp}(r)$

$$un_x+vn_r=0 \quad (1.5)$$

$$\left(\frac{\partial v}{\partial x}+\frac{\partial u}{\partial r}\right)(n_r^2-n_x^2)+2\left(\frac{\partial u}{\partial x}-\frac{\partial v}{\partial r}\right)n_xn_r=0 \quad (1.6)$$

$$p=p_a-\left(\frac{1}{R_1}+\frac{1}{R_2}\right)T+2\left[\frac{\partial u}{\partial x}n_x^2+\frac{\partial v}{\partial r}n_r^2+\left(\frac{\partial v}{\partial x}+\frac{\partial u}{\partial r}\right)n_xn_r\right] \quad (1.7)$$

where $F_{\mp}(r)$ represent the functions of the free surfaces, n_x, n_r, R_1, R_2 are components x and r of unit vector normal to free surface and their principal radii of curvature. They have the following relations with $F_{\mp}(r)$:

$$n_{x_{\mp}}=\pm\frac{1}{\sqrt{1+F_{\mp}'^2}},\ \ n_{r_{\mp}}=\mp\frac{F'_{\mp}}{\sqrt{1+F_{\mp}'^2}},\ \ \left(\frac{n_r}{n_x}\right)_{\mp}=-F'_{\mp} \quad (1.8)$$

$$\frac{1}{R_1}+\frac{1}{R_2}=|F''_{\mp}(1+F_{\mp}'^2)^{-3/2}|+|F'(1+F'^2)^{-1/2}r^{-1}| \quad (1.9)$$

If the free surfaces are spherical, then

$$\frac{1}{R_1}+\frac{1}{R_2}=2\,|F''_{\mp}(1+F'^2_{\mp})^{-3/2}| \tag{1.10}$$

Thereafter we assume spherical free surfaces, so that (1.10) holds. It should be pointed out, that due to the assumption of infinite thin liquid layer remained at the wall $r=1$ on the free surface are singularities. At these points velocity can take any value in the interval from $-U$ to free surfaces.

Both equations (1.2) and the boundary conditions (1.3)—(1.7) are nonlinear. It is difficult to solve it analytically or numerically. For the sake of simplification we linearize the nonlinear boundary conditions. Assume that the free surfaces are close to straight lines. Therefore, $F_{\mp}$, $F'_{\mp}$ are small compared to unity, but $F''_{\mp}$ is still the quantity of zero order, thus surface tension which play an important role in capillary flow is retained. The boundary conditions (1.5), (1.6) (1.7) are now satisfied at $x=\mp\lambda$ rathdr than on free surface. Neglecting the small quantity of higher order, we have:

$$u=-1,\quad v=0 \quad \text{for } r=1 \tag{1.11}$$

$$v=0 \qquad \text{for } r=0 \tag{1.12}$$

$$\left.\begin{aligned} &u=0 &(1.13)\\ &\frac{\partial v}{\partial x}=0 &(1.14)\\ &p=p_a-2T\,|F''_{\mp}|+2\frac{\partial u}{\partial x} &(1.15)\end{aligned}\right\}\ \text{for } x=\mp\lambda$$

Linearization of the boundary conditions on the free surface leads to considerable simplification of the problem. Now, velocity, pressure and free surface are separated. At first one may solve u, v, p, from equation (1.2) and boundary conditions (1.11)—(1.14) and then solve $F_{\mp}$ from (1.15) using u and p.

Assess the magnitude of Reynolds number in considered problem. In the following we present two sets of experimental data.

(1) Water is the fluid medium, capillary is glass-blown. Thus $\mu=0.01\text{g/cm}\cdot\text{sec}$, $\rho=1\text{g/cm}^3$, $g=980\text{cm/sec}^2$, $T'=72.5$ dyne/cm, $\alpha=10°$, $P'_a=1.013\times10^6$dyne/cm. By the experimental data at $a=0.021$ cm, velocity of descent U/U_∞ versus dimensionless length of liquid column $\lambda=L/a$ is shown in Table 1. Take account of the fact that at $\lambda=\infty$ there is Poiseuille flow in all the capillary, gravity is balanced with viscous force. Then $G=8=\dfrac{ga^2}{\nu U_\infty}$. It results that $U_\infty=5.402$, for $\lambda=\infty$. Figure 3 plots U/U_∞ versus λ.

Table 1

λ	5	10	20	30	∞
U(cm/sec)	1	1.75	3	4	5.40
G	43.22	14.70	14.40	10.80	8
T	7250	4143	2417	1813	1342
Re	2.1	3.7	6.3	8.4	11.3

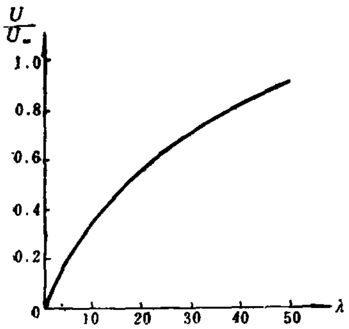

Fig. 3

(2) Blood is the working fluid and the capillary is glassmade. Then $\mu = 0.04$g/cm·sec, $g = 980$cm/sec^2, $\rho = 1.055$g/cm, surface tension $=$ 54dyne/cm, $\alpha = 48°$. By experimental results we have $U = 0.53$ for $\lambda = 18$. Correspondingly, $Re = 0.7$, $G = 115.6$, $T = 2641.50$.

It is evident that in our problem Reynolds number is not very high, usually it is less than 100. Hence we can restrict our study, first of all, at low Reynolds number and then consider the inertial effect.

II. Analytic Solution at Low Reynolds Number

In the case of low Reynolds number inertia term can be neglected. Eq. (1.2) becomes.

$$\left.\begin{aligned} &\frac{\partial u}{\partial x} + \frac{1}{r}\frac{\partial (rv)}{\partial r} = 0 \\ &\nabla p = G\vec{e}_x + \nabla^2 \vec{v} \end{aligned}\right\} \tag{2.1}$$

where $\vec{e}_x$ is the unit vector in x direction, $\vec{v}$ is the velocity vector. First of all we abstract the hydrostatic pressure $G(x+\lambda)$ and surface tension $p_a - 2T\cos\alpha$, providing equilibrium from pressure expression, where α is the angle of contact between liquid and wall in the state of equilibrium. Later we separate the velocity profile of Poiseuille flow $u_0 = -1 + 2(1 - r^2)$ from the velocity expression. In consonance with that it must be subtracted $-8(x+\lambda)$ from pressure expression. Considering all above, we have:

$$\left.\begin{aligned} &u = -1 + 2(1 - r^2) + u' \\ &v = v' \\ &p = (G - 8)(x + \lambda) + p_a - 2T\cos\alpha + p' \\ &\psi = -\frac{r^2}{2}(1 - r^2) + \psi' \end{aligned}\right\} \tag{2.2}$$

where u', v', p', ψ' are velocity components of circulating current, pressure and stream function respectively. Substituting (2.2) into (2.1) and (1.11)—(1.15), it leads to:

$$\left.\begin{aligned} &\frac{\partial u'}{\partial x}+\frac{1}{r}\frac{\partial(rv')}{\partial r}=0 \\ &\nabla p'=\nabla^2\vec{v}' \end{aligned}\right\} \tag{2.3}$$

$$u'=0 \quad \text{for } r=1 \tag{2.4}$$

$$v'=0 \quad \text{for } r=1 \tag{2.5}$$

$$v'=0 \qquad \text{for } r=0 \tag{2.6}$$

$$u'=-(1-2r^2) \tag{2.7}$$

$$\frac{\partial v'}{\partial x}=0 \qquad \text{for } x=\mp\lambda \tag{2.8}$$

$$p'=-(G-8)(x+\lambda)+2T\cos\alpha-2T|F''_{\mp}|+2\frac{\partial u'_0}{\partial x} \tag{2.9}$$

Introduce function f' which satisfies the following equations:

$$u'=-\frac{1}{r}\frac{\partial}{\partial r}\left(r\frac{\partial f'}{\partial r}\right) \qquad v'=\frac{\partial^2 f'}{\partial r\partial x}$$

Therefore, equation of continuity is satisfied identically. Rewrite $\vec{v}'$ into the following form:

$$\vec{v}'=-\vec{e}_x\frac{1}{r}\frac{\partial}{\partial r}\left(r\frac{\partial f'}{\partial r}\right)+\vec{e}_r\frac{\partial^2 f'}{\partial r\partial x}=\nabla\frac{\partial f'}{\partial x}-\vec{e}_x\nabla^2 f'$$

where $\vec{e}_x$, $\vec{e}_r$ are unit basic vectors in x and r directions. When it is substituted into the second equation in (2.3). one obtains:

$$\nabla p'=\nabla\nabla^2\frac{\partial f'}{\partial x}-\vec{e}_x\nabla^4 f' \tag{2.10}$$

Eq. (2.10) is satisfied if

$$\left.\begin{aligned} &\nabla^4 f'=0 \\ &p'=\nabla\frac{\partial f'}{\partial x} \end{aligned}\right\} \tag{2.11}$$

Now we must solve the biharmonic equation

$$\nabla^4 f'=0 \tag{2.12}$$

When f' is obtained, u', v', p' and stream function ψ' can be determined by the following formulas:

$$\left.\begin{aligned} &u'=-\frac{1}{r}\frac{\partial}{\partial r}\left(r\frac{\partial f'}{\partial r}\right) \qquad v'=\frac{\partial^2 f'}{\partial r\partial x} \\ &p'=\nabla^2\frac{\partial f'}{\partial r} \qquad\qquad\qquad \psi'=r\frac{\partial f'}{\partial r} \end{aligned}\right\} \tag{2.13}$$

It is obvious that our flow variables are symmetrical or antisymmetrical about axis r. As it has been done in paper [1], a solution of (2.12), which satisfies the conditions (2.4) and (2.8), can be found:

$$f'(x,r)=\sum_{n=1}^{\infty}A_n\left[\left\{-[2+k_n\lambda\tanh k_n\lambda]\frac{\cosh k_nx}{\cosh k_n\lambda}+k_nx\frac{\sinh k_nx}{\cosh k_n\lambda}\right\}\frac{J_0(k_nr)}{k_n^2J_1(k_n)}\right.$$
$$\left.+\sum_{m=1}^{\infty}B_{nm}\cos p_mx\left\{\frac{I_0(p_mr)}{p_m^2I_0(p_m)}-\frac{rI_1(p_mr)}{p_m[2I_0(p_m)+p_mI_1(p_m)]}\right\}\right] \quad (2.14)$$

where A_n and B_{nm} are arbitrary constants, J_i and I_i denote the ith order Bessel functions and modified Bessel functions of the first kind respectively, k_n is the nth root of the equation $J_0(x)=0$, $p_m=\frac{(m+1/2)\pi}{\lambda}$.

When (2.14) is substituted into (2.13), one obtains the following equations for the x and r components of the velocity:

$$u'=\sum_{n=1}^{\infty}A_n\left[\left\{-[2+k_n\lambda\tanh k_n\lambda]\frac{\cosh k_nx}{\cosh k_n\lambda}+k_nx\frac{\sinh k_nx}{\cosh k_n\lambda}\right\}\frac{J_0(k_nr)}{J_1(k_n)}\right.$$
$$\left.-\sum_{m=1}^{\infty}B_{nm}\cos p_mx\left\{\frac{I_0(p_mr)}{I_0(p_m)}-\frac{2I_0(p_mr)+p_mrI_1(p_mr)}{2I_0(p_m)+p_mI_1(p_m)}\right\}\right] \quad (2.15)$$

$$v'=\sum_{n=1}^{\infty}A_n\left[\left\{[1+k_n\lambda\tanh k_n\lambda]\frac{\sinh k_nx}{\cosh k_n\lambda}-k_nx\frac{\cosh k_nx}{\cosh k_n\lambda}\right\}\frac{J_1(k_nr)}{J_1(k_n)}\right.$$
$$\left.-\sum_{m=1}^{\infty}B_{nm}\sin p_mx\left\{\frac{I_1(p_mr)}{I_0(p_m)}-\frac{p_mrI_0(p_mr)}{2I_0(p_m)+p_mI_1(p_m)}\right\}\right] \quad (2.16)$$

Using the orthogonality relations of sine functions $\sin p_mx$, one finds:

$$B_{nm}=\frac{4k_n^3}{\lambda(k_n^2+p_m^2)^2}\frac{\sin\left(m+\frac{1}{2}\right)\pi}{\frac{I_1(p_m)}{I_0(p_m)}-\frac{p_mI_0(p_m)}{2I_0(p_m)+p_mI_1(p_m)}} \quad (2.17)$$

We shall determine the constants A_n with boundary condition (2.7). By applying the orthogonality properties of Bessel functions we have:

$$A_n=-\frac{1}{k_n}+\frac{8}{k_n^3} \quad (2.18)$$

It is easy to verify that condition (2.6) is satisfied identically. Therefore a solution of biharmonic eq. (2.14), which satisfies all boundary conditions, is found. A_n and B_{nm} in this expression are determined by (2.17) and (2.18), respectively.

The pressure p' and the stream function ψ' can be obtained from (2.13):

$$p' = \sum_{n=1}^{\infty} A_n\left[2k_n \frac{\sinh k_n x}{\cosh k_n\lambda}\frac{J_0(k_n r)}{J_1(k_n)} + \sum_{m=1}^{\infty} B_{nm} p_m \sin p_m x \frac{2I_0(p_m r)}{2I_0(p_m) + p_m I_1(p_m)}\right] \quad (2.19)$$

$$\psi' = \sum_{n=1}^{\infty} A_n\left[\left\{-[2 + k_n\lambda\tanh k_n\lambda]\frac{\cosh k_n x}{\cosh k_n\lambda} + k_n x\frac{\sinh k_n x}{\cosh k_n\lambda}\right\}\frac{-rJ_1(k_n r)}{k_n J_1(k_n)} + \sum_{m=1}^{\infty} B_{nm}\cos p_m x\left\{\frac{rI_1(p_m r)}{p_m I_0(p_m)} - \frac{r^2 I_0(p_m r)}{2I_0(p_m) + p_m I_1(p_m)}\right\}\right] \quad (2.20)$$

having u', v', p' and ψ', u, v, p and ψ can be calculated with (2.2).

The forms of the upper and lower meniscuses are determined by applying the condition (2.9). Obviously, that

$$|F''_-| = \cos\alpha + \frac{1}{2T}\left[-p'_- + 2\frac{2u'}{\partial x_-}\right] \quad (2.21)$$

$$|F''_+| = \cos\alpha - \frac{2}{2T}\left[-2\lambda(G-8) - p'_+ + 2\frac{\partial u'}{\partial x_+}\right] \quad (2.22)$$

Taking $|F''_-| = -F''_-$, $|F''_+| = F''_+$, $F(1) = 0$, $F'(0)$ into account and integrating (2.21) and (2.22), one obtains:

$$F_-(r) = -\frac{\cos\alpha}{2}(r^2-1) - \frac{1}{2T}[D(r) - D(1)] = -\frac{\cos\alpha}{2}(r^2-1) + F_C(r) \quad (2.23)$$

$$F_+(r) = \frac{\cos\alpha}{2}(r^2-1) + \frac{\lambda}{2T}(G-8)(r^2-1) - \frac{1}{2T}[D(r) - D(1)] = \left[\frac{\cos\alpha}{2} - \frac{\lambda}{2T}(G-8)\right](r^2-1) + F_C(r) \quad (2.24)$$

where $F_C(r) = -\frac{1}{2T}[D(r) - D(1)]$ is deviation of meniscuses due to circulating current and

$$D(r) = \sum_{n=1}^{\infty} A_n\left[\{2\tanh k_n\lambda(2 + k_n\lambda\tanh k_n\lambda) - 2k_n\lambda\}\frac{A(k_n r)}{k_n J_1(k_n)} + \sum_{m=1}^{\infty} B_{nm}\sin\left(m + \frac{1}{2}\right)\pi\left\{\frac{6B(p_m r) + 2C(p_m r)}{p_m[2I_0(p_m) + p_m I_1(p_m)]} - \frac{2B(p_m r)}{p_m I_0(p_m)}\right\}\right] \quad (2.25)$$

$$\left.\begin{aligned} A(v) &= \iint_0^v [J_0(v)dv]dv \\ B(v) &= \iint_0^v [I_0(v)dv]dv \\ C(v) &= \iint_0^v [vI_1(v)dv]dv \end{aligned}\right\} \quad (2.26)$$

In the process of deduction we use the properties $p'_- = p'_+$ and $\frac{\partial u'}{\partial x_-} = -\frac{\partial u'}{\partial x_+}$.

It is worthwhile to indicate that dimensionless velocity and pressure profiles are independent on the properties of liquid and geometric parameters of tube, while the form of free surface is seriously dependent upon it. In what follows we shall first of all calc ulate the velocity and pressure profiles which are applied to whatever liquid, and later we shall determine the form of free surface for both water and blood.

Numerical results for velocity, pressure and shear stress are obtained for four different cases of λ: 2, 5, 10, 20, 30. In the calculation we take $n=30$, $m=60$. It is sufficient to carry out the calculation for half of the liquid column due to symmetry of u', ψ' and antisymmetry of v', p'.

The results of the calculation show that the circulating current occurs mainly within one radius distance from the free surface, out of which it is rapidly vanished and the velocity profile is nearly a Poiseuille flow. For example at a distance from the free surface, velocity profile is 99% of the Poiseuillian. It follows that, effect of the free surface on flow motion is remarkable only within one radius distance from it. In order to emphasize on the circulating current, flow patterns, velocity, pressure and shear stress profiles are plotted merely in the region from the free surface to the location that is one radius distance out of it (here results of calculation at $\lambda=5$ are employed. Results at another λ is nearly the same as at $\lambda=5$). Fig. 4 presents sketch of eleven dimensionless velocity

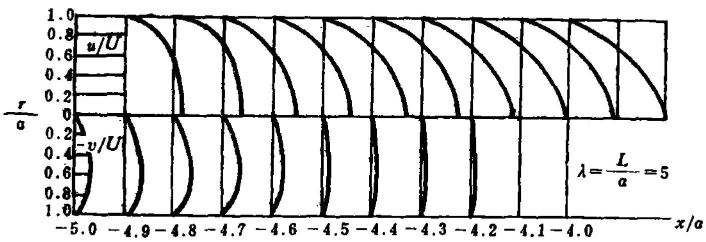

Fig. 4

profiles in the region $-5 \leqslant \lambda \leqslant -4$ with respect to the coordinate system fixed with the wall of capillary. Examining the sketch of $\frac{u}{U}$ and $-\frac{v}{U}$, it is found that the basic forms of these velocity profiles are similar to the bolus flows. The only difference between them is: in bolus flow $x=\mp\lambda$ are walls, at which velocity of fluid motion must be vanished, while in our problem $x=\mp\lambda$ are free surfaces, at which $u=0$ but v can take nonzero value. Therefore the intensity of $\frac{v}{U}$ at $x=\mp\lambda$ is stronger than bolus flow. Concretely speaking, the maximum velocity of $\frac{v}{U}$ reaches 0.54, while in bolus flow it only goes to 0.3. Furthermore, velocity of the circulating current has its maximum value on the free surface, while velocity of bolus flow which approaches to $x=\mp\lambda$ must be gradually decreased and finally it becomes to zero. So it is not difficult to understand that the length of space enough to develop the flow into Poiseuillian profile in our case it is shorter than that in bolus flow. For example, in our problem $\frac{u}{U}=$ 1.98 at $x=-\lambda+1$ while in bolus flow it has the value about 1.7.

The streamlines in left part of liquid column relative to the observed which is fixed with respect to the capillary and liquid column both are sketched in Fig. 5. In the coordinate system fixed with liquid column the circulating current can be seen clearly. The streamlines in the coordinate system fixed with capillary are bulged outward at $x=-\lambda$.

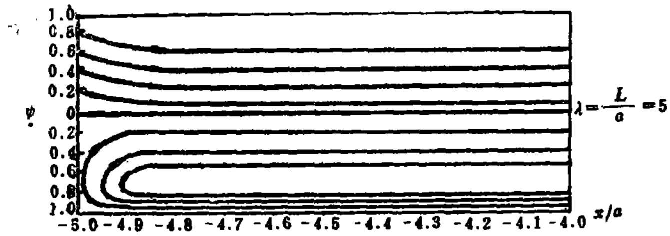

Fig. 5

Fig. 6 depicts shear stress and pressure profiles. Near the meniscus the shear stress at the wall is greater than that of the Poiseuillian one, while near the axis it is smaller. Pressure distribution is consistent with circulating velocity v. As r moves toward axis, the pressure continuously decreases. It is this pressure gradient which causes the occurrence of circulating velocity v. Both pressure gradient and v reach the maximum value at the meniscus.

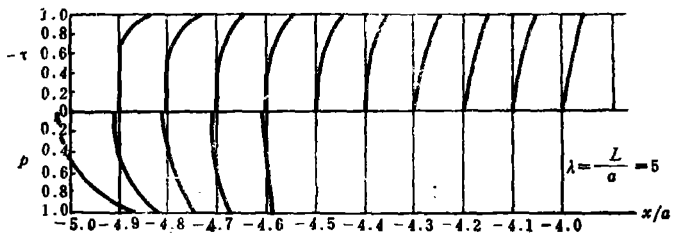

Fig. 6

Finally, we discuss the forms of upper and lower menisci which are related to properties of fluid and geometry of capillary. We distinguish two cases—water and blood.

(1) Water

Using the data in Table 1 and executing the calculation, one obtains

Table 1

r	0	0.1	0.2	0.3	0.4	0.5	0.6	0.7	0.8	0.9	1
$F_C(r)$	0.001	0.001	0.001	0.001	0.001	0.001	0.001	0	0	0	0

It is interesting to note that within the accuracy of 0.001, $F_C(r)$ is independent of λ. Viz. $F_C(r)$ have same results for $\lambda=2, 5, 10, 20, 30$. According to (2.23) and (2.24), $F_C(r)$ bends in the upper meniscus and flats in the lower. But the shift, which is much smaller than $\frac{\cos\alpha}{2}=0.492$, can be entirely ignored. On that account, we propose the following approximate formulas to determine the form of meniscuses with proper accuracy.

$$F_-(r) = -\frac{\cos\alpha}{2}(r^2-1) \tag{2.27}$$

$$F_+(r) = \left[\frac{\cos\alpha}{2} - \frac{\lambda}{2T}(G-8)\right](r^2-1) \tag{2.28}$$

From these formulas the following results are obtained:

λ	5	10	20	30
α_-	10°	10°	10°	10°
α_+	16.15°	19.18°	21.29°	20.20°

(2) Blood

Substitute the data of blood illustrated in section one into (2.27), (2.28) giving:

$$\alpha_- = 48°, \qquad \alpha_+ = 85.26°$$

Hence, the upper meniscus is principally the same one as that which is in equilibrium and the lower one must be modified by gravity and Poiseuillian pressure.

III. Inertial Effect

Consider the nonlinear inertial effect, viz if the inertial terms in the left sides of eqs. (1.2) are retained, what will be brought about in the solutions?

It is very difficult to solve the eqs. (1.2) analytically under the boundary conditions (1.11)—(1.15). In what follows we apply the effective time-dependent method in finite-difference techniques to solve this problem. With the stream function ψ and the vorticity ζ as dependent variables. the governing equations and boundary conditions for unsteady fluid motion may be expressed as:

$$\frac{\partial\zeta}{\partial t}+\frac{\partial(u\zeta)}{\partial r}+\frac{\partial(v\zeta)}{\partial r}=\frac{1}{Re}\left(\frac{\partial^2\zeta}{\partial x^2}+\frac{\partial^2\zeta}{\partial r^2}+\frac{1}{r}\frac{\partial\zeta}{\partial r}-\frac{\zeta}{r^2}\right) \tag{3.1}$$

$$\frac{\partial^2\psi}{\partial x^2}+\frac{\partial^2\psi}{\partial r^2}-\frac{1}{r}\frac{\partial\psi}{\partial r}=-r\zeta \tag{3.2}$$

$$\psi=0 \text{ at } r=1 \tag{3.3}$$

$$\psi=0, \quad \zeta=0 \text{ at } r=0 \tag{3.4}$$

$$\psi=0, \quad \zeta=0 \text{ at } x=\mp\lambda \tag{3.5}$$

where

$$\zeta=\frac{\partial v}{\partial x}-\frac{\partial u}{\partial r}, \qquad u=\frac{1}{r}\frac{\partial\psi}{\partial x}, \qquad -v=\frac{1}{r}\frac{\partial\psi}{\partial x} \tag{3.6}$$

The stresses are determined in terms of the velocity gradients:

$$\tau_{rr}=2\frac{\partial v}{\partial r}, \quad \tau_{xx}=2\frac{\partial u}{\partial x}, \quad \tau_{\theta\theta}=2\frac{v}{r}, \quad \tau_{xr}=\tau_{rx}=\frac{\partial v}{\partial x}+\frac{\partial u}{\partial r} \tag{3.7}$$

The second upwind differencing scheme are used for advection terms in (3.1)[2]. Hence equation (3.1) can be written in the following finite-difference form:

$$\zeta_{i,j}^{k+1}=\zeta_{i,j}^{k}-\Delta t\,(ADQR+ADQX)+\frac{\Delta t}{Re}\left(\frac{\zeta_{i+1,j}+\zeta_{i-1,j}-2\zeta_{i,j}}{\Delta x_i^2}\right.$$

$$\left.+\frac{\zeta_{i,j+1}+\zeta_{i,j-1}-2\zeta_{i,j}}{\Delta r_j^2}+\frac{\zeta_{i,j+1}-\zeta_{i,j-1}}{2r_j\Delta r_j}-\frac{\zeta_{i,j}}{r_j^2}\right) \tag{3.8}$$

where

$$ADQR = \frac{v_R\zeta_R - v_L\zeta_L}{\Delta r}, \quad v_R = \frac{v_{j+1} + v_j}{2}, \quad v_L = \frac{v_j + v_{j-1}}{2}$$

$$\zeta_R = \begin{cases} \zeta_j & v_R > 0 \\ \zeta_{j+1} & v_R < 0 \end{cases} \qquad \zeta_L = \begin{cases} \zeta_{j-1} & v_L > 0 \\ \zeta_j & v_L < 0 \end{cases}$$

$$ADQX = \frac{u_R\zeta_R - u_L\zeta_L}{\Delta x}, \quad u_R = \frac{u_{i+1} + u_i}{2}, \quad u_L = \frac{u_i + u_{i-1}}{2}$$

$$\zeta_R = \begin{cases} \zeta_i & u_R > 0 \\ \zeta_{i+1} & u_R < 0 \end{cases} \qquad \zeta_L = \begin{cases} \zeta_{i-1} & u_L > 0 \\ \zeta_i & u_L < 0 \end{cases}$$

here $\zeta^k_{i,j}, \zeta^{k+1}_{i,j}$ designate the ζ value which is referred to (i, j) point at k time level and $k+1$ time level, respectively. Equation (3.2) for ψ is solved by using "successive overrelaxation" method. Its corresponding finite-difference equation is:

$$\psi^{k+1}_{i,j} = (1-\omega)\psi^k_{i,j} + \omega\left\{\frac{1}{2(1+\beta^2_{i,j})}(\psi^k_{i+1,j} + \psi^{k+1}_{i-1,j} + \beta^2_{i,j}\ \psi^k_{i,j+1} + \beta^2_{i,j}\ \psi^{k+1}_{i,j-1}\right.$$

$$\left. - \frac{\Delta x_i \beta_{i,j}}{2r_j}\ \psi^k_{i,j+1} + \frac{\Delta x_i \beta_{i,j}}{2r_j}\ \psi^{k+1}_{i,j-1} + r_j \Delta x^2_i \zeta_{i,j}\right\} \tag{3.9}$$

where $\beta_{i,j} = \frac{\Delta x_i}{\Delta r_j}$, ω is relaxation factor.

The procedure of time-dependent method to solve steady fluid motion can be formulated as follows:

(1) The intervals in x and r directions are divided into i and j equal mesh spacing. To ensure stability of the scheme, time step must be chosen to be less than Δt_{crit}:

$$\Delta t_{crit} = \frac{1}{\frac{2}{Re}\left(\frac{1}{\Delta x^2} + \frac{1}{\Delta r^2}\right) + \frac{|u|_{max}}{\Delta x} + \frac{|v|_{max}}{\Delta r}}$$

(2) Take the solutions at low Reynolds number as the initial distribution. Once the new ζ distribution in mesh system subtracted from the boundary nodes at time $t = \Delta t$ is obtained from (3.8), the new ψ distribution at time Δt is found from (3.9) by iteration until the change in the stream-function value at each point in the field is not greater than 10^{-5}. The boundary condition for ψ gives the value of ψ at the boundary nodes. All of them is equal to zero.

(3) Equation

$$\zeta_{i,j}=\frac{1}{\Delta r_j}-\frac{\psi_{j-2}}{2\Delta r_j^2 r_{j-1}}$$

is used to obtain the vorticity on the solid boundary (the vorticity on other boundaries are known from boundary conditions). Velocity components u and v are then computed from (3.6). Now, all physical quantities at time Δt are computed.

(4) The previous procedure is continued until the change in the total vorticity of the fluid is of the order of 3×10^{-3} or less. We assume that this is the time required to reach the "steady state".

Numerical computations were being performed using the previous method for $\lambda=2$ and $Re=24.5$. A regular mesh containing 201×41 points was used ($i=201$, $j=41$). The solutions at low Reynolds number were taken as the initial values. Δt was 0.01sec. Relaxation factor equals 1.75. Computational experiment shows that the solutions approach very rapidly to the steady state. After four time levels the relative change in the total vorticity was less than 0.003. All physical quantities at two neighbouring time have three equal figures. Now we consider this in terms of our solution for the steady motion.

Nonlinear velocity profiles at $Re=24.5$ and $\lambda=2$ are shown in Fig. 7. In the same figure the linear one is sketched for the sake of comparison.

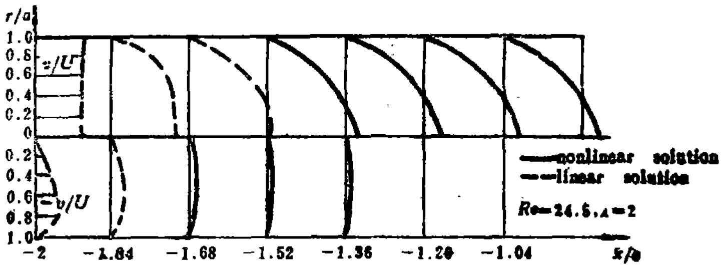

Fig. 7

This figure clearly demonstrates that the difference between the nonlinear and linear solutions is very small provided $Re=24.5$. Maximum shift occurs at the free surface. Both velocity profiles at another section are nearly coincided with each other. It follows that the inertial effect can be ignored at $Re\leqslant24.5$.

The following table shows the u, v, ψ values computed at $Re=24.5$ and $\lambda=2$ within one radius distance from the meniscus. Nonlinear solutions are unsymmetrical with respect to axis r. But the unsymmetrical behaviour is not serious, so only numerical results at upper meniscus are presented.

Table 2

u/U

	−2	−1.84	−1.68	−1.52	−1.36	−1.20	−1.04	−0.88
0	0.00000	0.36658	0.64876	0.82259	0.91103	0.94953	0.96485	0.97094
0.1	0.00000	0.36359	0.64110	0.81016	0.89516	0.93173	0.94621	0.95202
0.2	0.00000	0.35436	0.61668	0.77132	0.84581	0.87664	0.88869	0.89367
0.3	0.00000	0.33864	0.57428	0.70478	0.76241	0.78455	0.79304	0.79683
0.4	0.00000	0.31485	0.51416	0.60700	0.64258	0.65439	0.65885	0.66126
0.5	0.00000	0.27948	0.42480	0.47169	0.48330	0.48496	0.48569	0.48676
0.6	0.00000	0.22568	0.29277	0.29135	0.28147	0.27521	0.27321	0.27317
0.7	0.00000	0.13877	0.10506	0.05892	0.03469	0.02451	0.02122	0.02034
0.8	0.00000	−0.01705	−0.16004	−0.23086	−0.25783	−0.26710	−0.27031	−0.27181
0.9	0.00000	−0.32875	−0.52006	−0.57754	−0.59454	−0.59890	−0.60126	−0.60331
1.0	−1.00000	−1.00000	−1.00000	−1.00000	−1.00000	−1.00000	−1.00000	−1.00000

v/U

	−2	−1.84	−1.68	−1.52	−1.36	−1.20	−1.04	−0.88
0	0.00000	0.00000	0.00000	0.00000	0.00000	0.00000	0.00000	0.00000
0.1	−0.09561	−0.08310	−0.05617	−0.03092	−0.01422	−0.00578	−0.00227	−0.00094
0.2	−0.18928	−0.16317	−0.10834	−0.05858	−0.02641	−0.01059	−0.00418	−0.00176
0.3	−0.27919	−0.23701	−0.15208	−0.07996	−0.03478	−0.01362	−0.00546	−0.00236
0.4	−0.36325	−0.30089	−0.18309	−0.09169	−0.03805	−0.01443	−0.00597	−0.00267
0.5	−0.43906	−0.34945	−0.19864	−0.09097	−0.03575	−0.01302	−0.00572	−0.00269
0.6	−0.50247	−0.37359	−0.18735	−0.07833	−0.02861	−0.00991	−0.00488	−0.00243
0.7	−0.55062	−0.35889	−0.15145	−0.05614	−0.01861	−0.00607	−0.00369	−0.00194
0.8	−0.56363	−0.28407	−0.09318	−0.02996	−0.00870	−0.00263	−0.00239	−0.00130
0.9	−0.57402	−0.13104	−0.03107	−0.00853	−0.00198	−0.00053	−0.00106	−0.00056
1.0	0.00000	0.00000	0.00000	0.00000	0.00000	0.00000	0.00000	0.00000

ψ/Ua^2

	−2	−1.84	−1.68	−1.52	−1.36	−1.20	−1.04	−0.88
0	0.00000	0.00000	0.00000	0.00000	0.00000	0.00000	0.00000	0.00000
0.1	0.00000	0.00183	0.00323	0.00409	0.00452	0.00471	0.00479	0.00482
0.2	0.00000	0.00721	0.01267	0.01596	0.01760	0.01829	0.01857	0.01868
0.3	0.00000	0.01588	0.02757	0.03444	0.03773	0.03909	0.03962	0.03984
0.4	0.00000	0.02734	0.04665	0.05745	0.06237	0.06431	0.06507	0.06540
0.5	0.00000	0.04075	0.06788	0.08181	0.08777	0.09001	0.09088	0.09128
0.6	0.00000	0.05473	0.08778	0.10293	0.10890	0.11099	0.11182	0.11225
0.7	0.00000	0.06679	0.10099	0.11450	0.11930	0.12083	0.12147	0.12187
0.8	0.00000	0.07196	0.09938	0.10829	0.11107	0.11184	0.11222	0.11253
0.9	0.00000	0.05886	0.07103	0.07414	0.07497	0.07514	0.07529	0.07545
1.0	0.00000	0.00000	0.00000	0.00000	0.00000	0.00000	0.00000	0.00000

IV. Conclnsion

(1) There are considerable circulating currents near the menisci. Maximum circulating velocity is about 57% of the average velocity of the mainstream.

(2) Domain of circulating current viz. domain of influence is mainly situated within one radius distance from the free surface, out of which there is Poiseuille flow.

(3) The effect of circulating current on meniscus is very weak. Upper meniscus is principally the same as it is in equilibrium and the lower one must be modified by gravity and Poiseuillian pressure.

(4) Inertial effect is not considerable and can be ignored provided $Re \leqslant 24.5$.

* * * * *

The authors are indebted to Prof. H. S. Tan for his care and encouragement. We are very grateful to Messrs. Xu Jian-jun, Chia Fu, Peng Rong-rui who kindly provided valuable comments in the discussion. We especially wish to thank Drs. Weng Wei-liang and Quan Mu-ying for their assistance in arrangement of the experiments which were carried out in Xi-yuan Hospital.

References

1. Lew, H. S. and Fung, Y. C., Biorheology 6 (1969) 109—119.
2. Roache, P. J., Computational Fluid Dynamics (1972),